Dalton Transactions

Accepted Manuscript

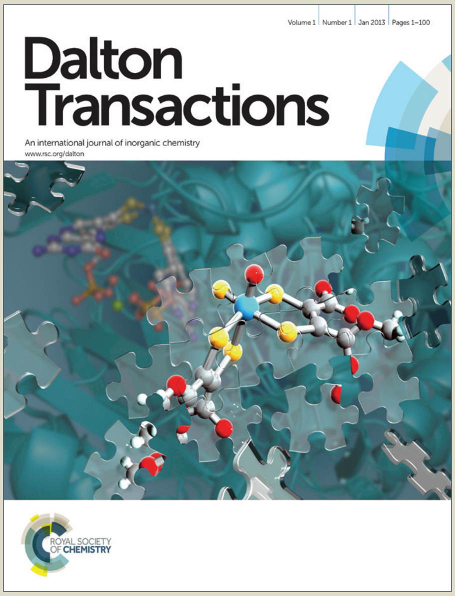

ROYAL SOCIETY OF CHEMISTRY

www.rsc.org/dalton

Cite this: DOI: 10.1039/c0xx00000x

www.rsc.org/xxxxxx

ARTICLE TYPE

$Ba_2B_{10}O_{17}$: A New Centrosymmetric Alkaline-Earth Metal Borate with Deep-UV Cut-Off Edge

Lili Liu, [a,b] **Xin Su,** [a] **Yun Yang,** [a*] **Shilie Pan,** [a*] **Xiaoyu Dong,** [a] **Shujuan Han,** [a] **Min Zhang,** [a] **Jing Kang,** [a,b] **Zhihua Yang** [a*]

Received (in XXX, XXX) Xth XXXXXXXXX 20XX, Accepted Xth XXXXXXXXX 20XX
DOI: 10.1039/b000000x

A new centrosymmetric alkaline-earth metal borate, $Ba_2B_{10}O_{17}$, has been successfully synthesized through high-temperature solid-state reactions. The single-crystal X-ray structural analysis shows that $Ba_2B_{10}O_{17}$ crystallizes in the triclinic space group $P\bar{1}$. The parameters of the triclinic unit cell are a = 6.7128(3) Å, b = 9.8698(4) Å, c = 9.9998(4) Å, α = 76.860(3)°, β = 83.200(3)°, γ = 73.332(3)°, and Z = 2. The title compound features a $[B_{10}O_{17}]_\infty$ three-dimensional anionic framework, with infinite channels in which the Ba^{2+} cations are located. $Ba_2B_{10}O_{17}$ processes a large experimental band gap of 6.29 eV, and a short cut-off edge lower than 180 nm proved by transmission spectrum on a single crystal samples 0.5 mm in thickness. The calculated band structures and the density of states of $Ba_2B_{10}O_{17}$ suggest that its indirect energy gap is 5.97 eV which coheres with the experimental result. The thermal behavior and IR spectrum of $Ba_2B_{10}O_{17}$ are also reported in this work.

Introduction

In the recent years, numerous works dealing with borates have been published concerning new compounds, physical properties of some borates as well as contributions to borate crystal chemistry. As we know, a boron atom will link with either three oxygen atoms to form a triangle $[BO_3]$ or four oxygen atoms to form a tetrahedron $[BO_4]$. And then $[BO_3]$ and $[BO_4]$ may be further linked by sharing bridging oxygen atoms to form isolated rings and cages or infinite chains, layers and networks,[1-3] for instance, $[B_3O_6]$, $[B_3O_7]$, $[B_5O_{10}]$ and so on, which determines the diversity of borate family.[4,5] Whereas the greater electronegativity between B atom and O atom, borate material may have a wide optical transmission window. Planar $[BO_3]$ unit is easy to be polarized, and this may make compounds possess a large birefringence or second harmonic generation (SHG) effect. So it is easy to get new compounds with various properties in borate family.[6] So far, a number of excellent borate compounds have been found,[7] e.g., β-BaB_2O_4 (β-BBO), LiB_3O_5 (LBO), CsB_3O_5 (CBO), $CsLiB_6O_{10}$ (CLBO), $KBe_2BO_3F_2$ (KBBF) and $Sr_2Be_2B_2O_7$ (SrBBO). Metal cations, such as the alkali/alkaline earth metal cations, often contribute to the cut-off edge shift to the UV region, because the $d - d$ or $f - f$ electronic transitions in the closed d or f orbits have negative influences on the energy band gap.[8] In addition, Ba^{2+} with large radius may also result in large structural distortion.[9] In barium borate family, some compounds have been known,[10] such as α-BBO, β-BBO, BaB_4O_7, BaB_8O_{13}, $Ba_2B_2O_5$, $Ba_3B_2O_6$. Among these compounds, the most famous example is β-BBO, well-known for its useful properties, which is widely used in the manufacture of SHG devices.[6a, 11] It is reasonable to believe that new materials with good properties might also exist in binary borates incorporating alkaline-earth metal Ba element. Based on this idea, we have started to deeply explore BaO-B_2O_3 system. After systematic experiments, we obtained a new centrosymmetric compound, $Ba_2B_{10}O_{17}$ with space group $P\bar{1}$.

In BaO-B_2O_3 system, a compound, $Ba_2B_{10}O_{17}$, has been reported by Keszler et al. in 2001, which crystallizes in the triclinic noncentrosymmetric space group $P1$ and its measured second-harmonic signal is about 0.5 KDP.[12] Herein, we reported a new centrosymmetric phase, $Ba_2B_{10}O_{17}$ which is different from the reference reported before. The synthesis, crystal structure, thermal behavior, IR spectrum, transmission spectrum and theoretical calculation of $Ba_2B_{10}O_{17}$ are reported in this work.

Experimental Section

Single crystal preparation. All reagents were of analytical grade. We obtained the single crystal of $Ba_2B_{10}O_{17}$ with the stoichiometric ratio. Stoichiometric mixture of $BaCO_3$ (39.48 g, 0.20 mol) and H_3BO_3 (61.83 g, 1.00 mol) was mixed homogeneously and transferred to a Pt crucible. The sample was gradually heated to 980 °C, and kept at this temperature for 48 h, and then cooled to 896 °C. After that, a platinum wire was promptly dipped into the melt. The temperature was kept at 896 °C for 36 h. When the growth of crystal ended, it was lifted out of the liquid surface and allowed to cool to room temperature at a rate of 10 °C/h. Actually, we obtained partially transparent crystal (Figure S1 in the Supporting Information) and it is confirmed that the obtained phase is $Ba_2B_{10}O_{17}$ (Figure S2 in the Supporting Information). Suitable crystal for X-ray diffraction (XRD) is selected under an optical microscope. The transparent crystal of $Ba_2B_{10}O_{17}$ is shown in Figure S3 in the Supporting Information.

Structure determination. A transparent block of $Ba_2B_{10}O_{17}$ crystal with dimensions 0.224 mm × 0.093 mm × 0.042 mm was selected and mounted on a glass fiber with epoxy for the structure determination. The crystal structure of $Ba_2B_{10}O_{17}$ was determined at room temperature by single-crystal XRD on an APEX II CCD diffractometer using monochromatic Mo Kα radiation (λ = 0.71073 Å) and integrated with the SAINT program.[13] And numerical absorption corrections were carried out using the SCALE program for area detector.[13] All calculations were performed with programs from the SHELXTL crystallographic software package.[14a] All of atoms were refined using full matrix least-squares techniques with anisotropic thermal parameters, and final least-squares refinement is on F_o^2 with data having $F_o^2 \geq 2\sigma(F_o^2)$. The structures were checked for missing symmetry elements by the program PLATON.[14b] Relevant crystallographic data and details of the experimental conditions for $Ba_2B_{10}O_{17}$ are summarized in Table 1. Atomic coordinates and the equivalent isotropic displacement parameters are listed in Table S1 in the Supporting Information, and interatomic bond lengths and angles for $Ba_2B_{10}O_{17}$ and the calculation of the valence balance are displayed in Tables S2 and S3 in the Supporting Information, respectively.

Table 1 Crystal data and structure refinement for $Ba_2B_{10}O_{17}$.

Empirical formula	$Ba_2B_{10}O_{17}$
Temperature	296(2) K
Crystal system, space group	Triclinic, $P\bar{1}$
Unit cell dimensions	a = 6.7128(3) Å α=76.860(3)°
	b = 9.8698(4) Å β=83.200(3)°
	c = 9.9998(4) Å γ=73.332(3)°
Volume	617.07(4) $Å^3$
Z, Calculated density	2, 3.524 Mg/m^3
Absorption coefficient	6.456 mm^{-1}
F(000)	596
Theta range for data collection	2.09 to 27.49°
Limiting indices	$-8 \leq h \leq 8$, $-12 \leq k \leq 11$, $-12 \leq l \leq 12$
Reflections collected / unique	8869 / 2778 [R(int) = 0.0376]
Completeness to theta = 27.49	98.30%
Data / restraints / parameters	2778 / 0 / 263
Goodness-of-fit on F^2	1.021
Final R indices $[F_o^2 > 2\sigma(F_o^2)]$ [α]	R_1 = 0.0243 wR_2 = 0.0562
R indices (all data)[α]	R_1 = 0.0299, wR_2 = 0.0601
Extinction coefficient	0.0035(4)
Largest diff. peak and hole (e·$Å^{-3}$)	0.805 and -0.958 e.$Å^{-3}$

[α] $R_1 = \Sigma||F_o| - |F_c||/\Sigma|F_o|$ and $wR_2 = [\Sigma w(F_o^2 - F_c^2)^2 / \Sigma w F_o^4]^{1/2}$ for $F_o^2 > 2\sigma(F_o^2)$

Solid-state syntheses. A polycrystalline sample of $Ba_2B_{10}O_{17}$ is prepared with solid-state reaction techniques. A stoichiometric mixture of $Ba(NO_3)_2$ (5.23 g, 0.02 mol) and H_3BO_3 (6.18 g, 0.1 mol) was ground and loaded into a platinum crucible. The mixture was preheated at 500 °C for 4 h. Then the temperature was raised to 850 °C and held at that temperature for 48 h with several intermediate grindings and mixings. The purity of the sample was checked by powder XRD (Figure S2 in the Supporting Information).

Powder X-ray diffraction. Powder XRD analysis of $Ba_2B_{10}O_{17}$ was performed at room temperature in the angular range of 2θ =10–70° with a scan step width of 0.02° and a fixed counting time of 1 s/step using an automated Bruker D2 X-ray diffractometer equipped with a diffracted beam monochromator set for Cu Kα radiation (λ = 1.5418 Å). The powder XRD patterns of $Ba_2B_{10}O_{17}$ (Figure S2 in the Supporting Information) match the one simulated from single-crystal XRD studies suggesting that we obtained the $Ba_2B_{10}O_{17}$ phase. The SHG measurements of the $Ba_2B_{10}O_{17}$ sample were performed on a pulse Nd: YAG laser with a wavelength of 1064 nm. There is no green light detected, indicating that the crystal structure we solved is correct.

Infrared spectroscopy. An infrared spectrum data were recorded on Shimadzu IR Affinity-1 Fourier transform infrared spectrometer in the range from 400 to 4000 cm^{-1} with a resolution of 2 cm^{-1}. The 6 mg of sample was mixed thoroughly with 500 mg of dried KBr.

Transmittance spectroscopy. Transmittance spectrum data of the $Ba_2B_{10}O_{17}$ crystal were measured at room temperature with a Shimadzu SolidSpec-3700DUV spectrophotometer. Data were collected in the wavelength range 165–3300 nm under a constant flow of nitrogen gas.

Thermal analysis. Thermal gravimetric analysis (TGA) and differential scanning calorimetry (DSC) were studied on a NETZSCH STA 449C instrument at a temperature range of 40–1000 °C with a heating rate of 5 °C min^{-1} under a constant flow of nitrogen gas.

Numerical calculation details. To gain insight into the nature of chemical bonding of $Ba_2B_{10}O_{17}$, its electronic structures were calculated by the first principles method. We performed density functional calculations using the CASTEP package[15] within the gradient generalized approximation (GGA) with the Perdew-Burke-Ernzerhof (PBE)[16] on the experimentally refined structure. The following valence configurations were implemented: Ba $5s^2 5p^6 6s^2$, B $2s^2 2p^1$ and O $2s^2 2p^4$, respectively. The structure of $Ba_2B_{10}O_{17}$ was not fully optimized, and self-consistent field calculation was employed with a convergence criterion of 10^{-5} a.u.. The electronic wave function was expanded in plane waves up to a cutoff energy of 540 eV, and Monk-horst-Pack[17] k-point mesh (3 × 2 × 2) centered at G in the Brillouin zone (BZ). The other calculating parameters used in the calculations and convergent criteria were set by the default values of the CASTEP code.

Results and Discussions

Structure description. $Ba_2B_{10}O_{17}$ crystallizes into a triclinic crystal system with a centrosymmetric space group of $P\bar{1}$. In the asymmetric unit, there are two crystallographically unique Ba atoms, ten crystallographically unique B atoms and seventeen crystallographically unique O atoms (Table S1, Figure S4 in the

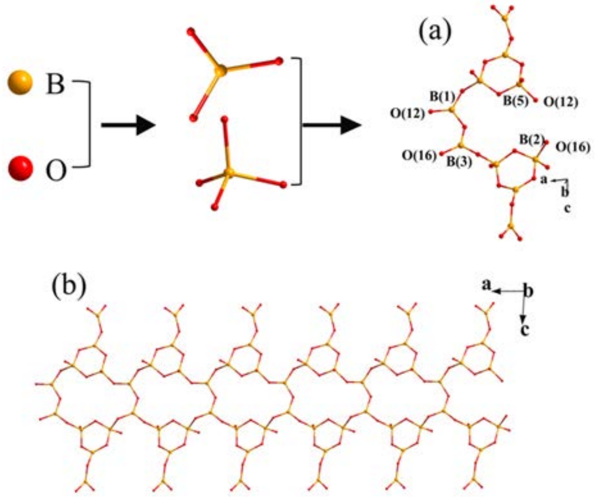

Figure 1 (a) The $[B_{10}O_{23}]$ unit. (b) Graph of the $[B_{10}O_{21}]_\infty$ chain projected along the *a*-axis.

Supporting Information). In terms of structure, B atoms are coordinated to either three O atoms to form planar $[BO_3]$ triangles, or four O atoms to form $[BO_4]$ tetrahedra. As shown in Figure 1a, six $[BO_3]$ triangles and four $[BO_4]$ tetrahedra interconnect via corner-sharing to form a fundamental building block (FBB) $[B_{10}O_{23}]$ unit. The $[B_{10}O_{23}]$ units build an infinite $[B_{10}O_{21}]_\infty$ chain along *a*-axis by $[B(1)O_3]$ sharing O(12) with $[B(5)O_4]$ and $[B(2)O_4]$ sharing O(16) with $[B(3)O_3]$ (Figure 1b). And two adjacent chains are oppositely parallel to each other and connected with each other by sharing O atoms to constitute three types of tunnels, A-type, B-type and C-type (Figure 2). For A-tunnel, as shown in Figure 3a, seen along *a*-axis, we can notice that the bridging atoms connecting the two adjacent oppositely parallel chains are O(9) atoms, and the tenfold coordinated Ba(1) atoms ($[Ba(1)O_{10}]$, Figure S5a in the Supporting Information) are located in this sort of tunnels (Figure 3b). In Figure 3c, we can catch sight of O(1) which is the bridging atom of B-tunnels, and elevenfold Ba(2) atoms in which two $[Ba(2)O_{11}]$ polyhedra form a $[Ba(2)_2O_{20}]$ dimer via edge-sharing (Figure S5b in the Supporting Information) dominate these tunnels (Figure 3d). A-tunnel connects with neighboring B-tunnel via sharing common O(2) and O(6), and by this way of connection, tunnels are linked with each other to constitute the whole $[B_{10}O_{17}]_\infty$ 3D network structure (Figures S6a and S6b in the Supporting Information). Apart from these, we can discover that a small C-typed tunnel is formed unintentionally in Figure S6a in the Supporting Information, and no any cations exist in it. Figure S6c in the Supporting Information exhibits the overall views of the $Ba_2B_{10}O_{17}$ down the *a*-axis.

In the structure of $Ba_2B_{10}O_{17}$, the existence of Ba atoms maintains the charge balance, and the Ba-O bond lengths have a wide region varying from 2.697(3) to 3.215(3) Å; B-O units determine the basic architecture of frame, and B-O bond lengths range from 1.347(5) to 1.504(5) Å. The results of bond valence calculations (Ba, 2.066–2.261; B, 2.972–3.088.) indicate that the Ba and B atoms are in oxidation states of +2 and +3, respectively (Tables S2 and S3 in the Supporting Information). These data demonstrated once again that the structure we solved is correct.

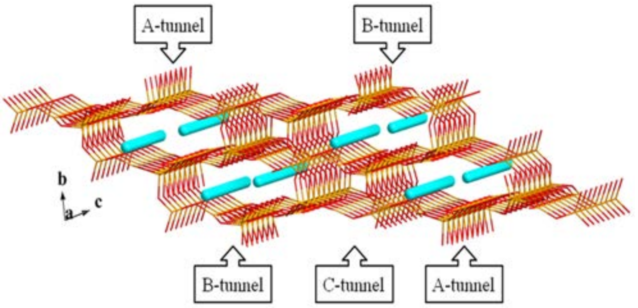

Figure 2 Perspective views of $Ba_2B_{10}O_{17}$ seen along *a*-axis.

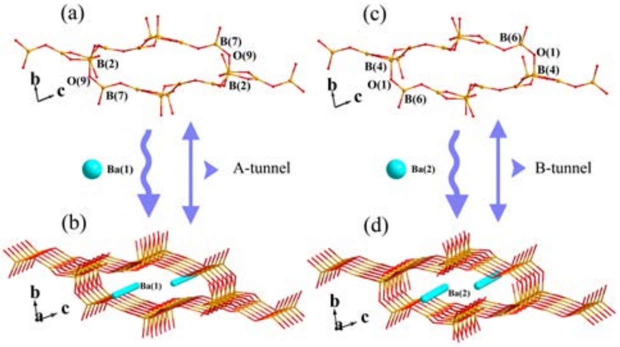

Figure 3 (a) Construction of A-tunnel. (b) Graph of A-tunnel seen along a-axis. (c) Construction of B-tunnel. (d) Graph of B-tunnel seen along a-axis.

Comparison among the compounds with $[B_{10}O_{17}]$ anion groups. By high-temperature solid-state reactions, compounds like $Na_2Tl_2B_{10}O_{17}$,[18] $Na_2Cs_2B_{10}O_{17}$[19] and $K_2Cs_2B_{10}O_{17}$[19] (the three compounds are isostructural and the unit cells are shown in Figure S7 in the Supporting Information) seem to have the same $[B_{10}O_{17}]$ anion group seen from their molecular formula. Compared with B-O units of these compounds, we found that the architecture of B-O unit in $Ba_2B_{10}O_{17}$ is different from them. $Na_2Tl_2B_{10}O_{17}$, $Na_2Cs_2B_{10}O_{17}$ and $K_2Cs_2B_{10}O_{17}$ crystallize in the monoclinic space group $C2/c$, and the title compound crystallizes in the triclinic space group $P\bar{1}$. They are different in architecture. The following will illuminate the structure with $Na_2Cs_2B_{10}O_{17}$ (NaCsBO) as an example.

In the structure of $Ba_2B_{10}O_{17}$, its B-O group regards $[B_{10}O_{23}]$ (Figure 1a) as the primitive cell, while NaCsBO chooses $[B_5O_{11}]$ unit (Figure 4a) as the minimum repeating cell. In the structure of NaCsBO, the $[B_5O_{11}]$ unit, consisting of three $[BO_3]$ and two $[BO_4]$, looks like a "∞"-shaped ring (Figure 4a). In Figure 4b, we can see that each $[B_5O_{11}]$ unit is linked with other units around it to form a 2D infinite layer of $[B_5O_9]_\infty$ via $[B(2)O_3]$ sharing O(2) with $[B(5)O_4]$ and $[B(3)O_3]$ sharing O(9) with $[B(5)O_4]$. Seen down the *b*-axis, the $[B_5O_9]_\infty$ layer is exhibited as the part circled by green line in Figure 4c. Two adjacent layers link with each other through sharing bridging O atoms among $[B(1)O_3]$ units to form a framework like sandwich which extends boundlessly on *b*-*c* plane (Figure 4c). Apparently, seen along *b*-axis, the adjacent sandwich frameworks do not link with each other directly (Figure 4d). It is the primary difference between B-O group of $Ba_2B_{10}O_{17}$

and B-O group of NaCsBO.

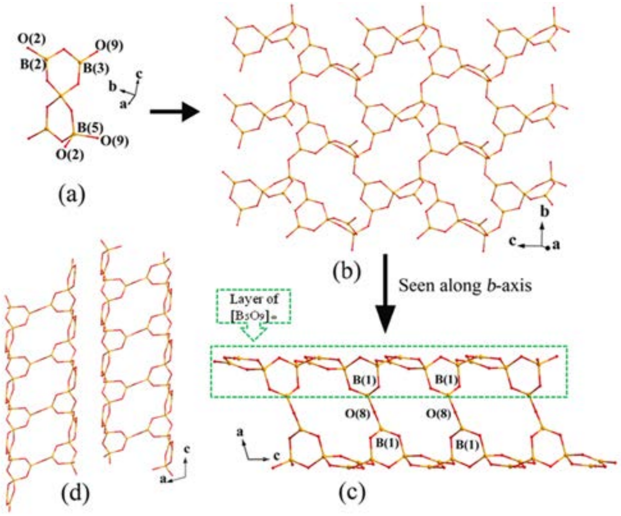

Figure 4 (a) The $[B_5O_{11}]$ group. (b) The $[B_5O_9]_\infty$ layer. (c) Graph of the sandwich structure of B-O group viewing along *b*-axis. (d) Graph of B-O group seen down *b*-axis in $Na_2Cs_2B_{10}O_{17}$ (B atom, yellow; O atom, red).

IR measurement. As shown in Figure S8 in the Supporting Information, there are three broad bands, which are around 1436, 1122, and 615 cm^{-1}, respectively. The broad band around 1436 cm^{-1} in the curve is attributed to the $[BO_3]$ asymmetric stretching vibrations, and the strong broad band around 1122 cm^{-1} is attributed to $[BO_4]$ asymmetric stretching vibrations. The absorption band around 615 cm^{-1} can be assigned to both the $[BO_3]$ and $[BO_4]$ bending modes. Therefore, the IR spectrum confirms the existence of trigonally and tetrahedrally coordinated boron atoms, which is consistent with the results obtained from the crystallographic data.[20]

Transmittance spectroscopy. Transmittance spectroscopy data of $Ba_2B_{10}O_{17}$ are exhibited in Figure S9 in the Supporting Information. It can be noticed that a wide transmission range is observed from 180 to 3000 nm, and the cut-off edge is below 180 nm, which indicates that the $Ba_2B_{10}O_{17}$ crystal may have potential use in deep-UV region. Figure S9 in the Supporting Information also shows that the experimental energy gap of $Ba_2B_{10}O_{17}$ is 6.29 eV.

Thermal behavior analysis. The TG and DSC curves of polycrystalline samples of $Ba_2B_{10}O_{17}$ are shown in Figure S10 in the Supporting Information. The results show that $Ba_2B_{10}O_{17}$ exhibits no weight loss up to 1000 °C. This illustrates that the compound is very stable. The DSC curve for $Ba_2B_{10}O_{17}$ exhibits one endothermic peak upon heating to 1000 °C which is at about 892 °C. The results demonstrate that $Ba_2B_{10}O_{17}$ may be a congruently melting compound. To verify the melting process, polycrystalline $Ba_2B_{10}O_{17}$ (5 g) was placed in a platinum crucible and heated to 950 °C, and then slowly cooled to room temperature. The solidified melt exhibits a diffraction pattern identical to that of the initial $Ba_2B_{10}O_{17}$ powder, as is shown in Figure S2 in the Supporting Information. This unambiguously demonstrates that $Ba_2B_{10}O_{17}$ is a congruently melting compound, and crystals of $Ba_2B_{10}O_{17}$ can thus be grown from its stoichiometric melt.

Band structures and density of states. As we know, the states close to the band gap dominate the optical properties of a crystal,[21] so we carefully analyzed the upper region of the valence band (VB) and the bottom of the conduction band (CB). Figure S11 in the Supporting Information is the calculated band structure along high-symmetry directions of Brillouin zone (Figure S12 in the Supporting Information) for $Ba_2B_{10}O_{17}$. From Table S4a in the Supporting Information, We can conclude that the conduction band minimum (CBM) is located at the Q point, and the valence band maximum (VBM) is at the G point, resulting in an indirect energy gap with a band gap of 5.97 eV, which is slightly smaller than the experimental value of 6.29 eV. Table S4b in the Supporting Information exhibits the calculated lattice constants (*a*, *b* and *c*) and angles (α, β and γ) between experimental and theoretical results for $Ba_2B_{10}O_{17}$.

The total and partial densities of states are shown in Figure S13 in the Supporting Information. As shown in Figure S13 in the Supporting Information, the density of states can be sorted into four major distinct regions, which exhibit several electronic characteristics: (1) Clearly, there exist peaks of 5*s* orbitals for Ba localized at about -24 eV. (2) The valence band (VB) between -21 and -16 eV mainly consists of 2*s*, 2*p* orbitals for oxygen, and 2*s*, 2*p* orbitals for boron. (3)The upper part of the VB from -10 to 0 eV is mainly composed of 2*p* orbitals of O atoms, and 2*s*, 2*p* orbitals of B atoms. There is a strong peak original from 5*p* orbitals of Ba atoms at -10 eV, but the top of the VB mostly consists of B-2*p* and O-2*p* orbitals. (4) The bottom of CBs is dominated by Ba-5*d* orbitals and the 2*p* orbitals of B and O atoms. It should be emphasized that the states on both sides of the band gap mainly consist of orbitals from the $[BO_n]$ anionic units. The transmission spectrum approaching deep-UV cut-off wavelength can be put down to the charge transfers mainly from O-*p* and B-*p* states below the Fermi level to the mixings of B-*p* and B-*s* states for $Ba_2B_{10}O_{17}$. In summary, the structure and composition of the $[B_{10}O_{17}]$ anionic groups determine the optical properties of the title compounds.

To gain more insight on the bonding character and explain the charge transfer in $Ba_2B_{10}O_{17}$, we have calculated the Mulliken population analysis. In the fourth column of Table S5 in the Supporting Information, the calculated bond charges of Ba-O and B-O bonds are 1.52–1.56 e, and 0.92–1.02 e (charge unit), respectively. It is obvious that the overlap populations have the following orders: BO_n (n=3, 4) > BaO_n (n=10, 11). The calculated bond orders for B-O (1.3618(1)–1.5040(0) Å) are in the range of 0.57–0.83 e; the bond orders for Ba-O (2.6964(4)–3.1749(5) Å) are in the range of -0.03–0.06 e (the fifth column of Table S5 in the Supporting Information). Hence, the results reveal that the covalent character of the B-O bonds is much larger than that of the Ba-O bonds, and the ionic character of Ba-O bonds is larger than that of the B-O bonds.[22] It is corroborated that some electrons from O-*p*, B-*p* and B-*s* states transfer into valence bands (VBs). Our calculated bond lengths show reasonable agreement with the experimental data (Table S5 in the Supporting Information).

Conclusions

A new centrosymmetric borate $Ba_2B_{10}O_{17}$ was synthesized by solid-state reactions and its crystallographic parameters and structure were defined. The title compound presents an intricate 3D network with $[B_{10}O_{23}]$ unit as FBB. And this network structure features three types of 3D tunnels: A- and B-type, which are filled with the Ba atoms; C-type, where no filler exists. Transmittance spectroscopy data indicate that this compound has a wide transmission range from 180 to 3000 nm and the UV cut-off edge is below 180 nm. Meanwhile, according to the theoretical calculation, it is confirmed that $Ba_2B_{10}O_{17}$ possesses an indirect band gap and a relatively large energy gap of 5.97 eV which is close to the experimental value of 6.29 eV. So this crystal may have potential as an optical material in deep-UV applications. We will continue to research the growth of large size crystals and the other optical properties in the future.

Acknowledgment

This work is supported by the National Natural Science Foundation of China (Grant Nos. 21101168, U1303193, 51302307, U1129301, 51172277), National Basic Research Program of China (Grant Nos. 2014CB648400, 2012CB626803), the "Western Light Foundation" Program of CAS (Grant No. XBBS201118), Main Direction Program of Knowledge Innovation of CAS (Grant No. KJCX2-EW-H03-03), the Funds for Creative Cross & Cooperation Teams of CAS, Major Program of Xinjiang Uygur Autonomous Region of China during the 12th Five-Year Plan Period (Grant No. 201130111), the High Technology Research & Development Program of Xinjiang Uygur Autonomous Region of China (Grant No. 201116143), the Science and Technology Project of Urumqi (Grant No. G121130002).

Notes and references

[a] *Key Laboratory of Functional Materials and Devices for Special Environments of CAS, Xinjiang Technical Institute of Physics & Chemistry of CAS, Xinjiang Key Laboratory of Electronic Information Materials and Devices, 40–1 South Beijing Road, Urumqi 830011, China. E-mail: yangyun@ms.xjb.ac.cn, slpan@ms.xjb.ac.cn (Shilie Pan)*

[b] *University of Chinese Academy of Sciences, Beijing 100049, China. Fax: (86)-991-3838957; Tel: (86)-991-3674558.*

† Electronic Supplementary Information (ESI) available: CCDC-number 981415 for $Ba_2B_{10}O_{17}$; CIF file; atomic coordinates and equivalent isotropic displacement parameters; selected bond lengths and angles; bond valence analysis; data of theoretical calculation; XRD patterns; photograph of the $Ba_2B_{10}O_{17}$ crystal; unit cell of $Ba_2B_{10}O_{17}$; the construction of $Ba_2B_{10}O_{17}$; the unit cells of $Cs_2K_2B_{10}O_{17}$, $Na_2Cs_2B_{10}O_{17}$ and $Na_2Tl_2B_{10}O_{17}$; IR spectrum and transmittance spectroscopy; the TG-DSC curves; calculated band structure and density of states; Brillouin zone of $Ba_2B_{10}O_{17}$.

1 (a) C. T. Chen, B. C. Wu, A. D. Jiang, B. C. Wu, G. M. You, R. K. Li and S. J. Lin, *J. Opt. Soc. Am. B*, 1989, **6**, 616; (b) H. W. Yu, H. P. Wu, S. L. Pan, Z. H. Yang, X. L. Hou, X. Su, Q. Jing, K. R. Poeppelmeier and J. M. Rondinelli, *J. Am. Chem. Soc.*, 2014, DOI: 10.1021/ja4117389; (c) H. P. Wu, H. W. Yu, S. L. Pan, Z. J. Huang, Z. H. Yang, X. Su and K. R. Poeppelmeier, *Angew. Chem. Int. Ed.*, 2013, **52**, 3406; (d) P. S. Halasyamani and K. R. Poeppelmeier, *Chem. Mater.*, 1998, **10**, 2753.

2 (a) S. L. Pan, Y. C. Wu, P. Z. Fu, G. C. Zhang, Z. H. Li, C. X. Du and C. T. Chen, *Chem. Mater.*, 2003, **15**, 2218; (b) H. P. Wu, H. W. Yu, Z. H. Yang, X. L. Hou, X. Su, S. L. Pan, K. R. Poeppelmeier and J. M. Rondinelli, *J. Am. Chem. Soc.*, 2013, **135,** 4215; (c) D. A. Keszler, A. Akella, K. I. Schaffers and T. Alekel, *Mater. Res. Soc. Symp. Proc*., 1994, **329**, 15.

3 (a) S. L. Pan, J. P. Smit, B. Watkins, M. R. Marvel, C. L. Stern and K. R. Poeppelmeier, *J. Am. Chem. Soc.*, 2006, **128**, 11631; (b) Y. Yang, S. L. Pan, H. Y. Li, J. Han, Z. H. Chen, W. W. Zhao and Z. X. Zhou, *Inorg. Chem.*, 2011, **50**, 2415; (c) F. Li, X. L. Hou, S. L. Pan and X. A. Wang, *Chem. Mater.*, 2009, **21**, 2846; (d) H. P. Wu, S. L. Pan, K. R. Poeppelmeier, H. Y. Li, D. Z. Jia, Z. H. Chen, X. Y. Fan, Y. Yang, J. M. Rondinelli and H. S. Luo, *J. Am. Chem. Soc.*, 2011, **133**, 7786.

4 (a) M. C. Chen, L. M. Wu, H. Lin, L. J. Zhou and L. Chen, *J. Am. Chem. Soc.*, 2012, **134**, 6058; (b) S. C. Wang and N. Ye, *J. Am. Chem. Soc.*, 2011, **133**, 11458; (c) H. P. Wu, H. W. Yu, S. L. Pan, A. Q. Jiao, H. Y. Li, J. Han, K. Wu and S. J. Han, *Dalton Trans.*, 2013, DOI:10.1039/C3DT53115E; (d) Y. Mori, I. Kuroda and S. Nakajima, *J. Cryst. Growth*, 1995, **156**, 307.

5 (a) Z. Wang, M. Zhang, S. L. Pan, Y. Wang and H. Zhang, *Dalton Trans.*, 2014, DOI: 10.1039/C3DT52592A; (b) M. Touboul, N. Penin and G. Nowogrocki, *Solid State Sci.*, 2003, **5**, 1327; (c) H. W. Yu, S. L. Pan, H. P. Wu, W. W. Zhao, F. F. Zhang, H. Y. Li and Z. H. Yang, *J. Mater. Chem.*, 2012, **22**, 2105; (d) S. C. Neumair, J. S. Knyrim, O. Oeckler, R. Glaum, R. Kaindl, R. Stalder and H. Huppertz, *Chem. Eur. J.*, 2010, **16**, 13659; (e) S. J. Chen, S. L. Pan, W. W. Zhao, H. W. Yu, H. P. Wu, Z. H. Yang and Y. Yang, *Dalton Trans.*, 2012**, 41**, 9202.

6 (a) P. Becker, *Adv. Mater.*, 1998, **10**, 979; (b) L. Cheng, Q. Wei, H. Q. Wu, L. J. Zhou and G. Y.Yang, *Chem. Eur. J.*, 2013, **19**, 17662.

7 (a) C. T. Chen, Y. B. Wang, B. C. Wu, K. C. Wu, W. L. Zeng and L. H. Yu, *Nature*, 1995, **373**, 322; (b) G. H. Zou, N. Ye, L. Huang and X. S. Lin, *J. Am. Chem. Soc.* 2011, **133**, 20001; (c) D. A. Keszler, *Curr. Opin. Solid State Mater. Sci.*, 1999, **4**, 155; (d) M. R. Marvel, J. Lesage, J. Baek, P. S. Halasyamani, C. L. Stern and K. R. Poeppelmeier, *J. Am. Chem. Soc*., 2007, **129**, 13963.

8 (a) M. Luo, N. Ye, G. H. Zou, C. S. Lin and W. D. Cheng, *Chem. Mater*., 2013, **25**, 3147; (b) T. T. Tran and P. S. Halasyamani, *Inorg. Chem.*, 2013, **52**, 2466; (c) C. Huang, C. L. Hu, X. Xu, B. P. Yang and J. G. Mao, *Inorg. Chem.*, 2013, **52**, 11551; (d) C. F. Sun, C. L. Hu, X. Xu, B. P. Yang and J. G. Mao, *J. Am. Chem. Soc.*, 2011, **133**, 5561.

9 C. T. Chen, N. Ye, S. J. Lin and Y. C. Wu, *Prog. Nat. Sci.*, 2000, **10**, 673.

10 P. P. Fedorov, A. E. Kokh and N. G. Kononova, *Russ. Chem. Rev.*, 2002, **8**, 651.

11 (a) C. T. Chen, B. C. Wu, A. D. Jiang and G. M. You, *Sci. Sin. B*, 1985, **28**, 235; (b) C. T. Chen, Y. C. Wu and R. K. Li, *J. Cryst. Growth*, 1990, **99**, 790; (c) K. Ogawa, T. Honma and T. Komatsu, *J. Solid State Chem.*, 2013, **207**, 6; (d) J. Lin, M. H. Lee, Z. P. Liu, C. T. Chen and C. Pickard, *Phys. Rev. B*, 1999, **60**, 13380.

12 J. L. Stone, D. A. Keszler, G. Aka, A. Kahn-Harari and T. A. Reynolds, *Proc. SPIE*, 2001, **4268**, 175.

13 SAINT, version 7.60A; Bruker Analytical X-ray Instruments, Inc.: Madison, WI, 2008.

14 (a) G. M. Sheldrick, SHELXTL, version 6.14; Bruker Analytical Xray Instruments, Inc. Madison, WI, 2008. 70; (b) A. L. Spek, *J. Appl. Crystallogr.*, 2003, **36**, 7.

15 S. J. Clark, M. D. Segall, C. J. Pickard, P. J. Hasnip, M. J. Probert, K. Refson and M. C. Payne, *Z. Kristallogr*., 2005, **220**, 567.

16 (a) L. Kleinman and D. M. Bylander, *Phys. Rev. Lett.*, 1982, **48**, 1425; (b) A. M. Rappe, K. M. Rabe, E. Kaxiras and J. D. Joannopoulos, *Phys. Rev. B*, 1990, **41**, 1227; (c) J. S. Lin, A. Qteish, M. C. Payne and V. Heine, *Phys. Rev. B*, 1993, **47**, 4174.

17 H. J. Monkhorst and J. D. Pack, *Phys. Rev. B*, 1976, **13**, 5188.

18 N. Penin, M. Touboul and G. Nowogrocki, *J. Alloys Compd.*, 2004, **363**, 104.

19 J. M. Tu and D. A. Keszler, *Inorg. Chem.*, 1996, **35**, 463.

20 (a) W. W. Zhao, S. L. Pan, J. Han, J. Y. Yao, Y. Yang, J. J. Li, M. Zhang, L. H. Zhang and Y. Hang, *J. Solid State Chem.*, 2011, **184**, 2849; (b) M. Zhang, S. L. Pan, J. Han, Y. Yang, L. Cui and Z. X.

Zhou, *J. Alloys Compd.*, 2011, **509**, 6696; (c) H. W. Yu, S. L. Pan, H. P. Wu, J. Han, H. Y. Li and Z. H. Yang, *Inorg. Chim. Acta*, 2012, **384**, 158.

21 M. H. Lee, C. H. Yang and J. H. Jan, *Phys. Rev. B*, 2004, **70**, 235110.

22 Y. Yang, X. Su, S. L. Pan, M. Zhang, Y. Wang, J. Han and Z. H. Yang, *CrystEngComm.*, 2014, **16,** 1978.

Table of contents

Manuscript title: $Ba_2B_{10}O_{17}$: A New Centrosymmetric Alkaline-Earth Metal Borate with Deep-UV Cut-Off Edge

$Ba_2B_{10}O_{17}$, a new barium borate, with band-gap of 5.97 eV, possesses a wide transmission range from 180 to 3000 nm.

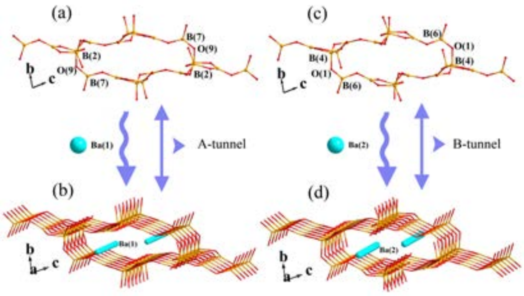

Abstract

A new centrosymmetric alkaline-earth metal borate, $Ba_2B_{10}O_{17}$, has been successfully synthesized through high-temperature solid-state reactions. The single-crystal X-ray structural analysis shows that $Ba_2B_{10}O_{17}$ crystallizes in the triclinic space group $P\bar{1}$. The parameters of the triclinic unit cell are a = 6.7128(3) Å, b = 9.8698(4) Å, c = 9.9998(4) Å, α = 76.860(3)°, β = 83.200(3)°, γ = 73.332(3)°, and Z = 2. The title compound features a $[B_{10}O_{17}]_\infty$ three-dimensional anionic framework, with infinite channels in which the Ba^{2+} cations are located. $Ba_2B_{10}O_{17}$ processes a large experimental band gap of 6.29 eV, and a short cut-off edge lower than 180 nm proved by transmission spectrum on a single crystal samples 0.5 mm in thickness. The calculated band structures and the density of states of $Ba_2B_{10}O_{17}$ suggest that its indirect energy gap is 5.97 eV which coheres with the experimental result. The thermal behavior and IR spectrum of $Ba_2B_{10}O_{17}$ are also reported in this work.